UNIVERSITÀ
DEGLI STUDI
DI PADOVA

Università degli Studi di Padova

Padua Research Archive - Institutional Repository

Gold(III)-pyrrolidinedithiocarbamato Derivatives as Antineoplastic Agents

(Article begins on next page)

Gold(III)–pyrrolidinedithiocarbamato Derivatives as Antineoplastic Agents**

Chiara Nardon,[a] Federica Chiara,[b] Leonardo Brustolin,[a] Alberto Gambalunga,[b] Francesco Ciscato,[c] Andrea Rasola,[c] Andrea Trevisan,[b] and Dolores Fregona*[a]

Transition metals offer many possibilities in developing potent chemotherapeutic agents. They are endowed with a variety of oxidation states, allowing for the selection of their coordination numbers and geometries via the choice of proper ligands, leading to the tuning of their final biological properties. We report here on the synthesis, physico-chemical characterization, and solution behavior of two gold(III) pyrrolidinedithiocarbamates (PDT), namely [$Au^{III}Br_2$(PDT)] and [$Au^{III}Cl_2$(PDT)]. We found that the bromide derivative was more effective than the chloride one in inducing cell death for several cancer cell lines. [$Au^{III}Br_2$(PDT)] elicited oxidative stress with effects on the permeability transition pore, a mitochondrial channel whose opening leads to cell death. More efficient antineoplastic strategies are required for the widespread burden that is cancer. In line with this, our results indicate that [$Au^{III}Br_2$(PDT)] is a promising antineoplastic agent that targets cellular components with crucial functions for the survival of tumor cells.

Introduction

Metal-based compounds have been largely used and studied as chemotherapeutic drugs since the discovery of the cytotoxic properties of cisplatin (cis-[$Pt(NH_3)_2Cl_2$]) in the late 1960s;[1–3] after its approval by the US Food and Drug Administration in 1978, cisplatin has become a milestone in antineoplastic treatment.[3,4] The therapeutic relevance of platinum-based compounds has led researchers to elucidate their mechanisms of action, with the aim to improve their efficacy on neoplasms and to hamper adverse reactions in healthy tissues.

It is known that the metal center in metal-based drugs is the pivotal moiety that acts as the anticancer "weapon", whereas the organic part of the molecule (ligand) plays other key roles, such as stabilizing the metal oxidation state, reducing systemic toxicity, and tuning water solubility. Under physiological-like conditions, metal centers, being positively charged, are favored to bind to negatively charged biomolecules, such as enzymes and nucleotides, or undergo redox processes.[5–8] On the other hand, the mechanism of biological action of metal compounds is, in several cases, not fully elucidated. As an example, in anti-cancer metallodrugs, DNA is not always the primary target as it appears for cisplatin.[6–9] In addition, the type of ligands (O-, N-, S-donors, monodentate or chelating ones, etc.), the nature, and the oxidation state of the metal center determine the hallmarks of the final compound such as its coordination geometry and stereochemistry and, ultimately, its biological behavior.[10–14] These observations, together with the poor toxicological profile of cisplatin, whose clinical use causes adverse effects and the occurrence of resistance,[15,16] have prompted the research into alternative platinum-based compounds, in order to find drugs with a better chemotherapeutic index in terms of toxicity–activity ratio.[15,17,18]

In the last years, we have broken into this research scene with our nonplatinum-based coordination compounds. These molecules are metal–dithiocarbamato (dtc) complexes potentially able to combine the cytotoxic activity of the related metal center (e.g. $Au^{I,III}$, $Ru^{II,III}$, Zn^{II}, Cu^{II}) with lack of toxicity owing to the inherent chemoprotective action of the dtc ligand.[19,20] Overall, our findings provide evidence for the importance of stabilizing the heavy metal center in order to prevent its nonspecific reactivity that would give rise to systemic toxicity.[21] Up to now, the most promising results have been obtained with gold(III) derivatives of the type [$Au^{III}X_2$(dtc)] (X = Cl, Br; dtc = various dithiocarbamato ligands). These compounds closely reproduce the structural features of cisplatin, and most of them are endowed with good anticancer activity, together with a very low or negligible systemic toxicity.[22–26]

In parallel to the synthesis of gold chemotherapeutics, we have also been synthetizing and studying coordination compounds of ruthenium and copper with pyrrolidinedithiocarba-

[a] Dr. C. Nardon, L. Brustolin, Prof. D. Fregona
Department of Chemical Sciences, University of Padova
Via F. Marzolo 1, 35131 Padova (Italy)
E-mail: dolores.fregona@unipd.it

[b] Dr. F. Chiara, Dr. A. Gambalunga, Prof. A. Trevisan
Department of Cardiac, Thoracic, and Vascular Sciences
University of Padova, Via Giustiniani 2, 35128 Padova (Italy)

[c] Dr. F. Ciscato, Dr. A. Rasola
Department of Biomedical Sciences, University of Padova
Viale G. Colombo 3, 35131 Padova (Italy)

mate (PDT) as a ligand. In this context, we found that the presence of PDT strongly affects the final biological activity. In fact, we recorded an encouraging cytotoxic activity in the nano and micromolar range against human non-small-cell lung cancer, two estrogen-receptor-α-positive breast cancer cell lines, the triple negative MDA-MB-231 breast cancer cell line, androgen-receptor-independent prostate tumor, ovarian and cervical squamous carcinoma cell lines, and the corresponding cisplatin-resistant subclones.[27,28] Therefore, in the present work we have combined the chelating ligand PDT with gold metal in a 1:1 metal-to-ligand stoichiometry with the remaining coordination sites occupied by two *cis*-halogen ions which may undergo hydrolysis in the physiological milieu.

In particular, we report on the synthesis of two new gold(III) pyrrolidinedithiocarbamates with the general formula [Au^{III}X$_2$(PDT)] as shown in Figure 1, wherein X is either Br (com-

[AuBr$_2$PDT]
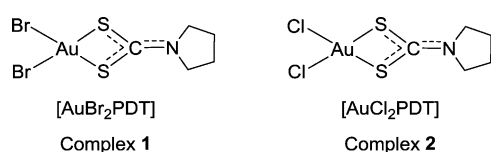Complex **1**

[AuCl$_2$PDT]
Complex **2**

Figure 1. Chemical structures of the synthesized gold(III) complexes.

plex **1**) or Cl (complex **2**). Their physico-chemical characterization was followed by the evaluation of their in vitro cytotoxicity on HeLa (cervical cancer), HCT116 (colon neoplasia), SAOS (osteosarcoma), and MEF-*NF1*$^{-/-}$ (immortalized primary embryonic fibroblast) cancer cell lines. The solution behavior of both complexes was also studied under physiological-like conditions by UV/Vis spectrophotometry. Then, the cell-death-inducing mechanisms were explored by investigating whether the compounds affect redox equilibrium or influence the mitochondrial permeability transition pore (PTP) activity.

Results and Discussion

Synthesis and characterization of the gold(III) complexes

Two gold(III)-pyrrolidinedithiocarbamato derivatives were prepared in very good yields via direct reaction of the salt ligand ammonium PDT with the metal precursor potassium tetrabromoaurate(III) or potassium tetrachloroaurate(III) under equimolar conditions at room temperature. The purity of all final compounds was higher than 95% (by thermogravimetric and elemental analysis). Both the starting ammonium PDT and the corresponding gold(III)-dithiocarbamato derivatives **1** and **2** (Figure 1) have been characterized by means of several techniques in order to confirm the expected stoichiometry as well as to investigate their structural features.

Elemental and thermogravimetric analyses highlighted a very good correlation between calculated and found values. In particular, thermal degradation primarily takes place via two steps, leading to the formation of metallic gold, in agreement with literature data[29,30] (Table 1). The presence of an endothermic differential scanning calorimetry (DSC) peak at about

Table 1. TG and DSC data for the gold(III)-dithiocarbamato compounds **1** and **2**.

Cmpd	Weight loss to Au(0) [%]		Peak temperature (process)[a] [°C]
	Calculated	Found	
1	−60.91	−60.95	261 (endo); 497 (exo); 1064 (endo)
2	−52.21	−51.91	242 (endo); 495 (exo); 1064 (endo)

[a] Endo = endothermic, exo = exothermic.

1064 °C (gold T_{melt}) along with no weight loss further confirms the decomposition to elemental gold. The first step is likely due to the formation of gold(I) thiocyanate upon reductive elimination as reported in literature for similar gold(III) dithiocarbamato compounds.[31,32]

The elucidation of the coordination mode and the strength of the bonds between the metal and the ligand donor atoms is of paramount importance in the characterization of metal derivatives designed for medicinal applications. In this regard, medium and far FT-IR spectroscopy are among the best diagnostic tools. Table 2 highlights that the band associated with

Table 2. Selected FT-IR frequencies of the ligand PDT and the corresponding gold(III)-dithiocarbamato compounds **1** and **2**.

Cmpd	Vibrational mode [cm^{-1}]				
	$\nu_{a/s}$ NH$_4^+$	ν N—CSS	$\nu_{a/s}$ SCS	$\nu_{a/s}$ SAuS	$\nu_{a/s}$ XAuX
NH$_4$(PDT)	3102[a]	1412	988/565	—	—
1	—	1583	943/537	411/371	240/218[b]
2	—	1586	942/538	413/375	362/315[c]

[a] NH$_4^+$; [b] X = Br; [c] X = Cl.

the N—CSS stretching shifts toward higher energies when passing from the free ligand to the corresponding gold derivatives due to an increased carbon–nitrogen double bond character following the coordination.[33–35] The detection of a single band at about 1000 cm^{-1}, attributable to the ν_a (S—C—S) for both gold(III) complexes, points out that the —NCSS moiety chelates the metal center in a symmetrical bidentate mode in agreement with our data on other complexes.[21,24,36] A band, detectable in the range 420–630 cm^{-1} and commonly ascribed to the ν_s (S—C—S) vibration, is observed for both the complexes and the free dithiocarbamato ligand (Table 2).[29,37–40] It is interesting to underline that this absorption is associated also with some $M\langle^S_S\rangle C$ ring deformations, as previously shown by detailed FT-IR isotopic studies on various dithiocarbamato complexes.[41] The presence of two new bands in the range 370–420 cm^{-1}, absent in the IR spectrum of the free ligand and ascribable to gold(III)–sulfur vibrations (ν_s and ν_a), further accounts for a chelated coordination geometry.[38] Notably, on the basis of the energies recorded for the $\nu_{a/s}$ (S—Au—S), compound **2** is characterized by a slightly stronger metal–ligand bond, which indirectly determines a higher stretching frequency for the N—CSS bond (Table 2).[42] Two halides complete the coordination sphere in

a *cis*-geometry as shown by the appearance of two new bands ($\nu_{a/s}$ (X—Au—X)) at 240/218 and 362/315 cm^{-1} for the complex **1** and **2**, respectively.[43,44] The other main frequencies, ascribable to the organic alkylic backbone, seem to be negligibly affected by metal coordination, except for the disappearance of the broad band at 3102 cm^{-1} ($\nu_{a/s}$ (NH$_4^+$)) (Table 2).

Concerning the NMR characterization, one and two-dimensional spectra (^{1}H,^{13}C HMBC, Table 3) showed an upfield shift (about 20 ppm with respect to the free ligand) for the signal

Table 3. ^{13}C NMR spectral data of the ligand PDT and compounds **1** & **2**.

Cmpd	δ [ppm]	
	R—N	—CSS
NH$_4$(PDT)	26.06 (*CH$_2$CH$_2$N*)	208.81
	53.00 (*CH$_2$CH$_2$N*)	
1	23.35 (*CH$_2$CH$_2$N*)	188.32
	50.87 (*CH$_2$CH$_2$N*)	
2	23.41 (*CH$_2$CH$_2$N*)	188.58
	51.10 (*CH$_2$CH$_2$N*)	

of the dithiocarbamato carbon atom for both complexes (at about 190 ppm), along with the disappearance of the NH$_4^+$ proton peak (at 7.33 ppm), confirming the formation of the gold(III) derivatives. In comparison with the spectrum recorded for ammonium PDT, all ^{13}C resonances are shifted at higher fields. Conversely, upon metal coordination the ^{1}H multiplets of all the methylene groups are shifted at lower fields, thus pointing out opposite shield effects on the two investigated NMR-active nuclei. By means of NMR kinetics, we checked the stability over time of both complexes in D$_6$-dimethylsulfoxide (DMSO) as predissolution of our hydrophobic compounds in this organic solvent is necessary to carry out the biological tests in cell culture medium.

UV/Vis spectrophotometric studies

When studying metallodrugs, it is necessary to test their stability under physiological conditions.[5] Therefore, detailed spectrophotometric studies were carried out for both complexes dissolved in DMSO (reference solvent) and saline solution. In order to better investigate the possible reactivity in both media, several electronic spectra were recorded up to 24 hours. It is worth pointing out that our compounds show a good antiproliferative activity already after a few hours of treatment.[22] Accordingly, in this work we highlight only the chemical and biological behavior after a three-hour treatment. The kinetic behavior of the coordination compounds **1** and **2** was first monitored in DMSO (Figure 2) at 37 °C and a concentration of 100 μM (main features collected in Table 4).

Table 4. Main absorption bands (evaluated at time zero) in the UV/Vis electronic spectra acquired in DMSO and saline solution at 37 °C.

Compound	Solvent	λ_{max} [nm]	
		Band 1	Band 2
1	DMSO	277.3	319.0
	Saline solution	269.3	311.6
2	DMSO	268.6	318.3
	Saline solution	269.2	311.1

Band 1 and band 2 have been ascribed in literature to intraligand $\pi^* \leftarrow \pi$ transitions mainly located in the —NCS and —CSS moieties, respectively.[29,38] Moreover, an intraligand $\pi^* \leftarrow n$ transition, where *n* is the in-plane nonbonding sulfur orbital, should be recorded at around 340 nm[45] but is not observable owing to the overlap with the more intense adjacent bands. A weak band at about 380 nm is visible only for the coordination compound **1** (labeled as band 3 in Figure 2) and is attributable to an intramolecular L←M charge transfer involving the M *nd* orbitals and the dithiocarbamato π^* system.[46,47] However,
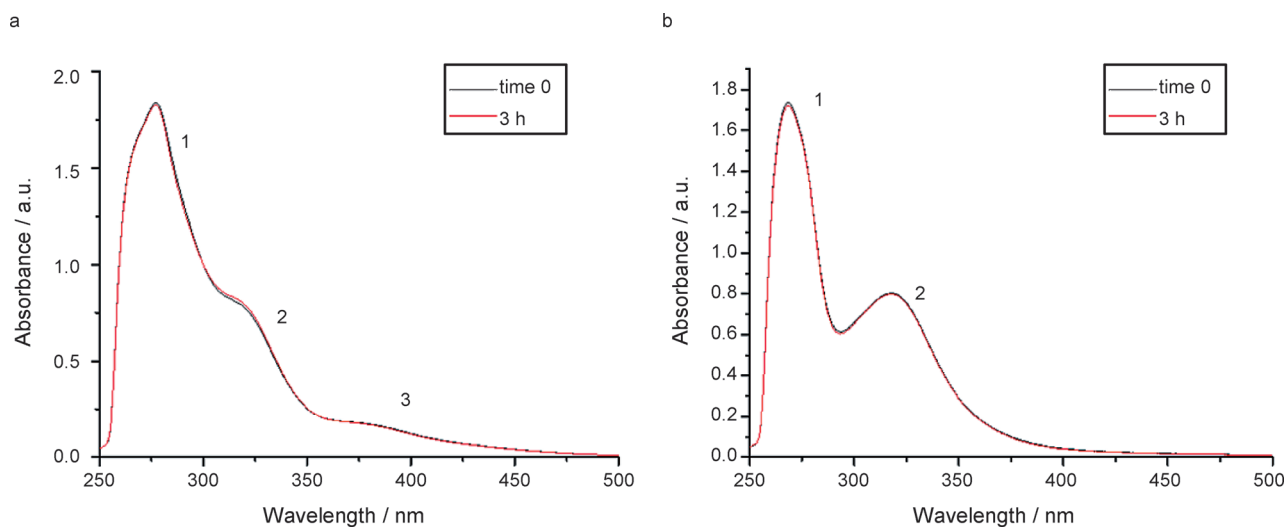

Figure 2. UV/Vis spectra recorded for compounds **1** (a) and **2** (b) in DMSO at 37 °C.

owing to the quite high oxidizing power of Au^{III}, this transition has been ascribed also to an electron transfer of the type $u \leftarrow g$ from a $4p$ orbital of the bromide ligands to the lowest unfilled $5d$ orbital of the metal center.[48] Its low intensity can be explained by a poor overlap between the $5d$ metal orbital and the involved $4p$ orbital (π symmetry).[48]

For both complexes, no major alteration of the bands related to the metal–ligand chromophore was observed over time. This behavior is likely due to the large stabilization effects brought about by the dithiocarbamato ligand. Such stability was further confirmed in the same solvent by ^{1}H NMR over three hours. On the basis of these results, DMSO was used to dissolve 1 and 2 prior to performing all the biological tests (< 0.5 % v/v) and was taken as reference medium in the discussion of the spectral features detected in saline solution. In this aqueous environment, the evolution with time was likewise followed by UV/Vis spectrophotometry for three hours at 37 °C (Figure 3), with both compounds being previously dissolved in DMSO (final concentration 100 μм, at 0.8 % and 1.3 % v/v content of DMSO for compound 1 and 2, respectively).

Table 4 reports only the absorption data recorded at the time zero. Similar to other our complexes,[14,49] contrary to DMSO medium, some decreases of the band intensities were quickly observed for both complexes upon dissolution in saline, reaching a steady condition after three hours. Overall, the maximum position of the bands is essentially unchanged over time. This points out that the gold center keeps the +3 oxidation state thanks to the stabilizing effects played by the chelating dithiocarbamato ligand.[50] The drop in spectral intensity can be ascribed to the progressive hydrolysis of gold(III)-bromide (compound 1) and gold(III)-chloride (compound 2) bonds, leading to the water-soluble aquo complexes and, ultimately, to the precipitation of the hydroxo derivatives (verified by elemental and far FT-IR analyses). In addition, compound 1 undergoes more rapid hydrolysis compared to the complex 2 with an absorbance decrease over one hour of about 11 % and 1 %, respectively, (Figure 3). This behavior highlights a higher intrinsic reactivity of the bromide derivative with respect to the chloride one under physiological-like conditions. In fact, bromide ranks lower than chloride within the experimental

spectrochemical series of ligands,[51] thus pointing out a greater capacity for the latter to cause d-orbital splitting. The larger the crystal field stabilization energy, the stronger the metal–ligand bond, in agreement with our previously described FT-IR data on the Au—X bond strength.

Biological assays

Compounds 1 and 2 induce dose-dependent tumor cell death

Treatment with both compounds 1 and 2 resulted in a rapid (three-hour) dose-dependent decrease of cell viability in the following human cancer cell lines: the highly aggressive SAOS-2 osteosarcoma cells, the HeLa cervical adenocarcinoma cells, the HCT116 colorectal carcinoma cells, and the mouse embryonic fibroblasts, obtained from mice where the bona fide tumor suppressor gene *NF1* was genetically ablated (MEF-*NF1*$^{-/-}$) (Table 5).

Table 5. Growth inhibition of various cell lines after 3 h treatment with the gold(III) compounds 1 and 2.

| Cmpd	IC$_{50}$[a] [μM]			
	SAOS-2	HeLa	HCT116	MEF *NF1*$^{-/-}$
1	12.2 ± 1.6	17.7 ± 1.6	15.8 ± 2.1	3.6 ± 0.9
2	26.4 ± 3.1	30.8 ± 4.2	43.6 ± 5.4	7.8 ± 1.1
Cisplatin	NE[b]	NE[b]	NE[b]	NE[b]

[a] Data represent the mean ± S.D. for n = 7. Cells tested were the following: human tumor cell lines SAOS-2 (human osteosarcoma), HeLa (cervical cancer), and HCT116 (colon neoplasia) and the immortalized primary mouse embryonic fibroblast (MEF) model MEF-*NF1*$^{-/-}$ (isolated from knockout strains for the oncosuppressor gene neurofibromine); [b] NE stands for not evaluable at 3 h treatment.

Our data also show that compound 1 is the most promising anticancer molecule, as it induced a markedly higher cytotoxicity than compound 2 in all tested cell types (Figure 4, a–d), suggesting that the presence of bromides instead of chlorides in the gold coordination sphere profoundly affects the biological efficacy of the potential drug. Cisplatin was tested as a refer-
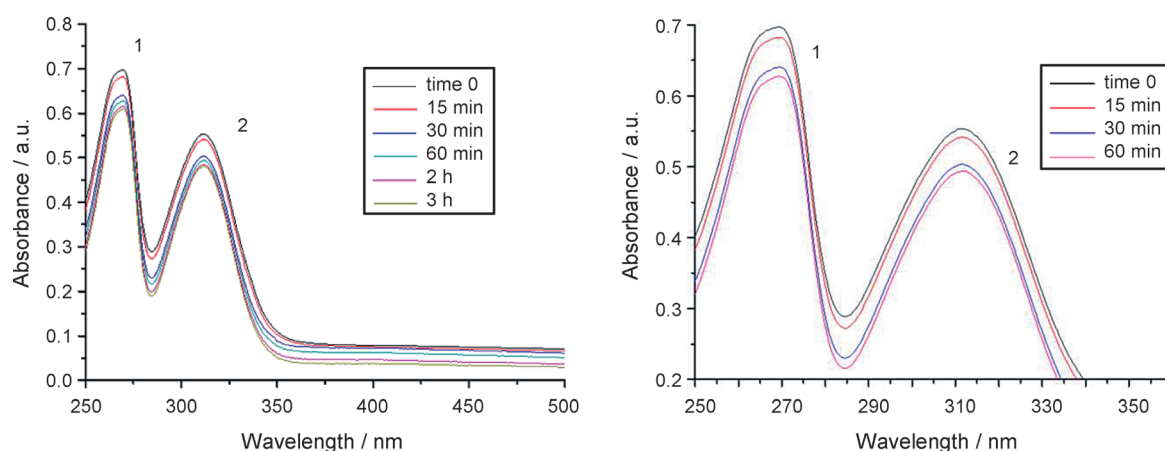
Figure 3. UV/Vis spectra recorded for compound 1 in saline solution at 37 °C over 3 h (left) and the first 60 min (right).
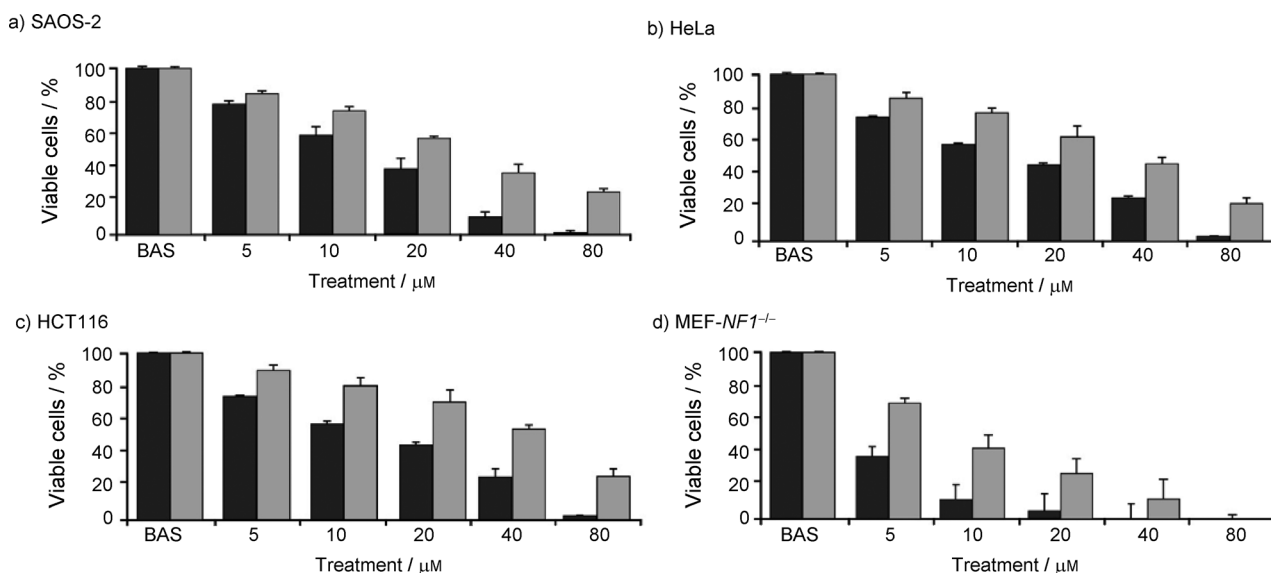
Figure 4. Compounds **1** (black bars) and **2** (grey bars) are cytotoxic to some cancer cell lines. Cell viability was measured on SAOS-2 (a), HeLa (b), and HCT116 (c) human cancer cell lines and on MEF-$NF1^{-/-}$ cells (d). Shown are dose-response experiments after a 3 h treatment with compounds **1** and **2**. BAS stands for the control. Values represent the mean ± S.D. of at least n = 7.

ence compound under the same experimental conditions recording no significant cytotoxicity after three hours of treatment.

Compound 1 increases intracellular reactive oxygen species (ROS) and sensitizes the permeability transition pore (PTP) to opening
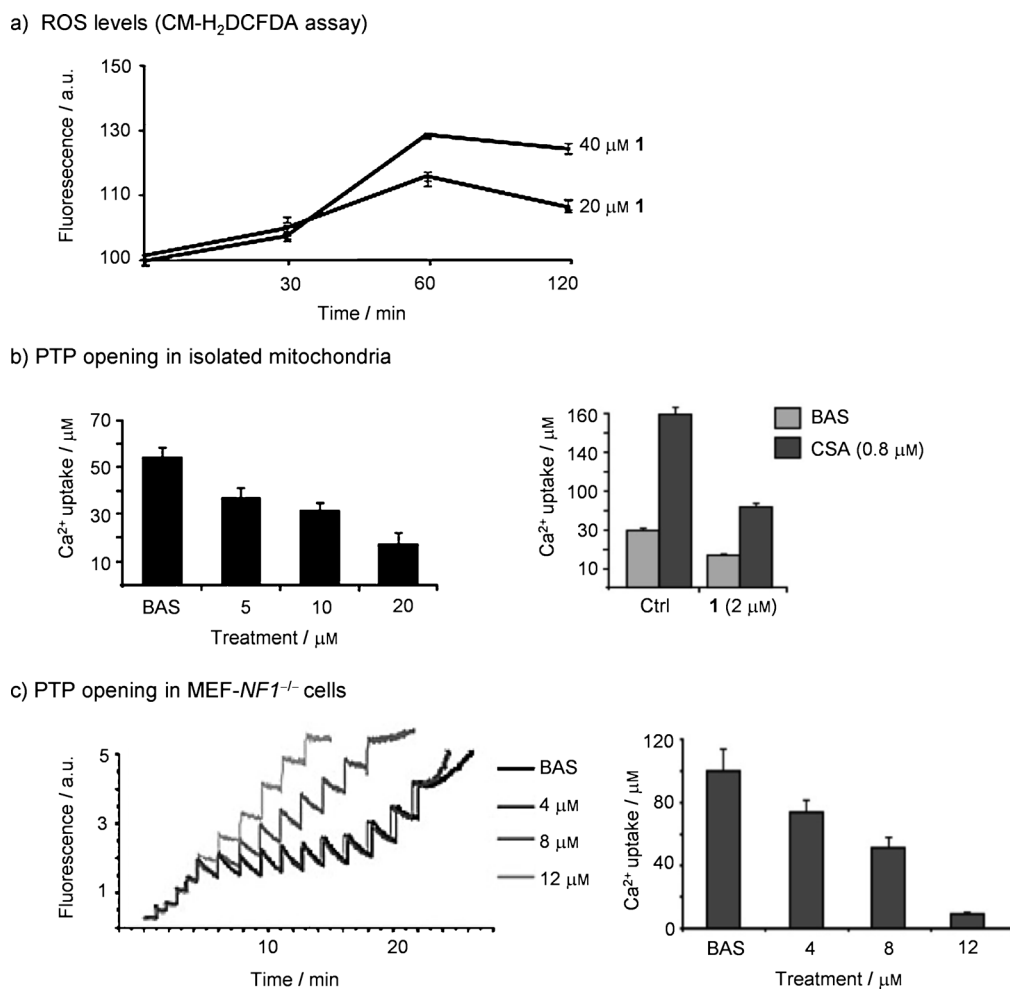
In the light of the antiproliferation screening, we then conducted the subsequent biological studies on the more active compound **1**.

Recently, we have shown[52] that the gold(III)-dithiocarbamato complex AuL12 causes a rise of mitochondrial superoxide levels that kills tumor cells by inducing ROS-dependent opening of the PTP. The PTP is a large channel located in the inner mitochondrial membrane, whose opening causes mitochondrial depolarization and swelling, leading to rupture of the outer mitochondrial membrane, release of Ca^{2+} and of pro-apoptotic proteins, and then cell death.[53, 54] Therefore, we evaluated whether the cytotoxicity elicited by compound **1** is mediated by a similar oxidative stress, which would prompt cell death by selectively triggering PTP opening in neoplastic cells. We performed these experiments on MEF-$NF1^{-/-}$, obtained from knockout mice for the onco-suppressor gene *NF1*. Such a gene encodes neurofibromin (Nf1), which negatively regulates Ras,[55] a master protooncogene whose hyperactivation is the most common oncogenic event, which prompts cell proliferation, apoptosis resistance, and metabolic rearrangements.[56] In addition to Ras hyperactivation, the ablation of the *NF1* gene also results in the genetic disease neurofibromatosis, characterized by the occurrence of diverse tumor types.[57] Based on these considerations, MEF-$NF1^{-/-}$ cells constitute a good model to check the antiblastic activity of our compounds.

The gold(III) compound **1** induced a rise in ROS levels (Figure 5 a). Kinetic experiments showed that the ROS increase was extremely rapid, reaching a maximum after 60 minutes (Figure 5 a). To ascertain whether compound **1** is capable of eliciting PTP opening, we performed a Ca^{2+} retention capacity (CRC) analysis, which evaluates PTP modulation in a semiquantitative way through the assessment of the amount of Ca^{2+} taken up by mitochondria before pore opening.[58] As shown in Figure 5 b, compound **1** triggered a dose-dependent CRC decrease on isolated liver mitochondria, which constitutes the standard model when setting CRC experiments, because hepatocytes are endowed with a high number of mitochondria. Inhibition of Ca^{2+} release from mitochondria by a control treatment of cyclosporine A (CSA), a well-known PTP inhibitor, confirmed that CRC experiments were assessing PTP modulation, and that the observed calcium release is due to PTP opening. These data suggest that compound **1** seems to promote cell death by inducing PTP opening, so we also carried out CRC experiments on the MEF-$NF1^{-/-}$ cells.[58] We found that a three-hour treatment with the gold(III) complex **1** caused a dose-dependent CRC shortening, that is PTP opening, on this cellular model as well (Figure 5 c). Furthermore, we performed parallel experiments in the presence of the ROS-scavenging compound Trolox, finding no changes in the effect of compound **1** on PTP opening. These experiments suggest that the cell death commitment induced by compound **1** is not only associated with its verified ability to induce ROS, but it is likely due to other ROS-independent pathways, that ultimately lead to PTP opening.

Conclusions

In the last four decades, the unquestionable therapeutic success of the anticancer drug cisplatin has prompted the design,

a) ROS levels (CM-H$_2$DCFDA assay)

b) PTP opening in isolated mitochondria

c) PTP opening in MEF-NF1$^{-/-}$ cells

Figure 5. Compound **1** is able to induce reactive oxygen species (ROS) and sensitize the permeability transition pore (PTP). a) Dose-response and ROS kinetics measured on mitochondria of MEF-NF1$^{-/-}$ treated up to 120 min with 20 μM and 40 μM of **1**; values represent the mean ± S.D. of at least n = 5. b) Left: changes on pore permeability transition induced by compound **1** on purified mitochondria from mouse liver and measured by calcium retention capacity (CRC). Right: same experiments carried out in the presence of the inhibitor cyclosporine A (CSA), added 1 h before treatment. Values represent the mean ± S.D. of at least n = 4. c) Left: example of a single experiment of PTP sensibility measured by a CRC assay on whole MEF-NF1$^{-/-}$ cells treated with different doses of **1**. Mitochondrial calcium uptake is plotted in terms of Calcium Green-5N fluorescence. Right: average histogram of the total Ca^{2+} uptake before PTP opening (error bars represent the S.D. for n = 3).

synthesis, and biological development of several metal-based potential chemotherapeutics. On the whole, our gold(III) complexes of the type [AuX$_2$(dtc)] (X = Cl, Br; dtc = various dithiocarbamates) stand out among others for their capability to strongly inhibit tumor growth both in vitro and in vivo by mechanisms of action differing from those recognized for the clinically-established platinum drugs.[59]

In this work, our novel compounds **1** and **2** showed a marked cytotoxicity towards different tumor cell types in a short treatment time (Table 5).

In order to exploit the chemotherapeutic potential of this class of gold(III) derivatives, it is mandatory to dissect their mode of action on target cells. One possibility is that tumor cell death is caused by oxidative stress. It must be underlined that malignant cells are extremely sensitive to oxidative stress as they are characterized by complex metabolic rearrangements, with an enhancement of glucose utilization and a concomitant decrease of mitochondrial respiration (the Warburg

effect[60–62]). As respiratory chain complexes are the major producers of ROS inside cells,[63] downmodulation of their activity enhances ROS generation, forcing cancer cells to set a novel homeostatic redox equilibrium by simultaneously inducing antioxidant defenses.[64] Thus, neoplasms might be sensitized to oxidative stress with respect to nontransformed tissues, as any increase in ROS levels could unbalance their redox equilibrium by overpowering their residual anti-oxidant capabilities.

In this research, we observed that the great activity of compound **1** on NF1$^{-/-}$ MEFs is paralleled by an increase in ROS levels. This oxidative assault is able to induce the PTP, a mitochondrial channel whose opening commits cells to death.[54] However, the presence of the scavenger Trolox does not affect the ability of compound **1** to trigger the pore transition in MEF-NF1$^{-/-}$ cells, thus suggesting the oxidative stress can only partially account for the efficacy of our potential drug. The chemical behavior of both complexes was also studied under physiological-like conditions by UV/Vis spectrophotometry in

order to gain insights into the stability of the gold(III) coordination sphere and to connect it with the degree of cytotoxicity of the compounds. In this regard, the organic/inorganic nature of the ligands can play a major role in modulating anticancer properties of the metal ion. On the whole, the analysis of the collected chemical data and their comparison with the biological results brings out a structure–activity relationship. In particular, we found that lability of the halogen–gold bond perfectly matches the biological effects of the complexes. In fact, it turned out that the faster the hydrolysis process of the Au–Br/Cl bond, the greater the chemotherapeutic effect observed, thus accounting for the stronger cytotoxicity of complex **1** in comparison with complex **2**. Such a phenomenon is in agreement with the findings reported by Casini et al. for other gold(III) anticancer agents.[5] In other words, our compounds undergo an "activation" process (i.e. release of one or both halide ligands from the tetracoordinated gold(III) center), required to react with the possible cellular targets and, hence, to trigger the antitumor effects. On the other hand, based on the redox properties (oxidizing) of the metal ion, a reductive step for the Au^{III} center cannot be ruled out a priori when studying the mechanism of action of this class of potential pharmaceuticals.

Experimental Section

Chemicals

KAuBr$_4$·2H$_2$O and KAuCl$_4$·2H$_2$O were purchased from Alfa Aesar, [D$_6$]DMSO from Aldrich, ammonium pyrrolidinedithiocarbamate from Fluka, and P$_4$O$_{10}$ from AnalaR Normapur–Prolabo. Dulbecco's modified Eagle medium (DMEM) was purchased from Euroclone. All other reagents and solvents (from Aldrich or Fluka) were of high purity and used without further purification. SAOS-2 osteosarcoma cells, HeLa cervical adenocarcinoma cells, and HCT116 colorectal carcinoma cells were purchased from the American Type Culture Collection (ATCC). MEF-$NF1^{-/-}$ cells were kindly provided by Prof. Reuven Stein (George S. Wise Faculty of Life Sciences, Tel Aviv University, Israel).

Instrumentation and general procedures

Elemental analysis was performed using a Carlo Erba 1108 CHNS-O microanalyser (CE Instruments Ltd., Wigan, UK).

FT-IR spectra were recorded at 298 K under N$_2$ atmosphere in Nujol between two polyethylene tablets on a Nicolet Nexus 870 FT-IR spectrophotometer (Nicolet Instrument Technologies, now Thermo Scientific, Waltham, USA) in the range 50–600 cm^{-1} (200 scansions, 4 cm^{-1} resolution), and in solid KBr on a Nicolet Nexus 5SXC FT-IR spectrophotometer (32 scansions, 2 cm^{-1} resolution) in the range 400–4000 cm^{-1}. Data processing was carried out using OMNIC version 5.1 (Thermo Scientific, Waltham, USA).

All 1D ^{1}H NMR and 2D spectra were acquired in [D$_6$]DMSO at 298 K on a Avance DRX300 spectrophotometer (Bruker, Billerica, USA) equipped with a broadband inverse (BBI) [^{1}H, X] probehead. Typical acquisition parameters for 1D ^{1}H NMR spectra (^{1}H: 300.13 MHz): 64–128 transients, spectral width 12 kHz, using 32 k data points and a delay time of 3.0 s. Spectra were processed by exponential weighting with a resolution of 0.5 Hz and a line-broad-

ening threshold of 0.1 Hz. Typical acquisition parameters for 2D [^{1}H,^{13}C] HMBC NMR spectra (^{1}H: 300.13/^{13}C: 75.48 MHz): 512 transients of 16 scans/block, spectral width 7.5/18.8 kHz, 1 k/1 k data points and a delay time of 2.0 s. Sequences were optimized for $^1J(^{13}C,^1H) = 145$ Hz/$^nJ(^{13}C,^1H) = 5$ Hz with no ^{1}H decoupling. Spectra were processed by using sine-square weighting with a resolution of 1.0/3.0 Hz and a line-broadening threshold of 0.3/1.0 Hz. Data processing was carried out by means of MestReNova version 6.2 (Mestrelab Research, Escondido, USA). Chemical shifts were referenced to the characteristic signal of the solvent by considering external tetramethylsilane (TMS).

Thermogravimetric (TG) and differential scanning calorimetry (DSC) curves were recorded on a thermobalance equipped with a DSC 2929 calorimeter (TA Instruments, New Castle, USA). Measurements were carried out in the range 25–1300 °C in alumina crucibles under air (flux rate 30 cm^3 min^{-1}) at a heating rate of 5 °C min^{-1}, using alumina as reference.

Electronic spectra were acquired at 37 °C in the range 250–500 nm using a Cary 100 UV/Vis double beam spectrophotometer (Agilent, Santa Clara, USA) (1 cm optical path, quartz cuvettes), using fresh solutions of the samples in DMSO. With respect to the studies in 0.9 % (w/v) NaCl solution, compounds **1** and **2** were dissolved in DMSO beforehand and subsequently diluted with saline solution (~1% v/v DMSO) to yield a final concentration of 100 μM. For the kinetic studies, the initial time (time zero) was set upon the complete dissolution of the complex.

Synthesis of the gold(III) complexes

To an aqueous solution of KAuX$_4$·2H$_2$O (X = Br, Cl; 0.6 mmol), the ligand NH$_4$(PDT) (0.6 mmol) was added dropwise while stirring at rt, giving rise to the immediate precipitation of a solid. After 10 min, the crude product was isolated by centrifugation (5,000 rpm, 15 min) and washed with H$_2$O and diethyl ether. Both complexes were then dried in vacuo in the presence of P$_4$O$_{10}$, with the final yield in the range of 85–90 %.

Dibromido[*N*-dithiocarboxy-$\kappa S, \kappa S'$-pyrrolidine]gold-(III) (Au^{III}Br$_2$(PDT), 1) Orange powder (89.6 %): soluble in DMSO, acetone, and dimethylformamide (DMF), slightly soluble in CH$_3$CN and CH$_2$Cl$_2$, insoluble in H$_2$O, EtOH, MeOH, isopropanol, CCl$_4$, and diethyl ether; FT-IR (KBr): $\tilde{v}_{max} = 2971–2849$ (v, CH$_2$), 1583 (v, N–CSS), 1447 (v, CH$_2$), 943 cm^{-1} (v_a, S–C–S); FT-IR (Nujol): $\tilde{v}_{max} = 537$ (v_s, S–C–S), 411 (v_a, S–Au–S), 371 (v_s, S–Au–S), 240 (v_a, Br–Au–Br), 218 cm^{-1} (v_s, Br–Au–Br); ^{1}H NMR (300.13 MHz, [D$_6$]DMSO, 298 K): $\delta = 2.06$ (m, 4H, CH_2CH$_2$N); 3.81 ppm (m, 4H, CH$_2$N); ^{13}C NMR (75.48 MHz, [D$_6$]DMSO, 298 K): $\delta = 23.35$ (CH$_2$CH$_2$N), 50.87 (CH$_2$N), 188.32 ppm (CSS); Anal. calcd for C$_5$H$_8$AuBr$_2$NS$_2$ (MW = 503.81): C 11.94, H 1.60, N 2.78, S 12.75, found: C 12.05, H 1.60, N 2.74, S 12.80; TG (air): calcd weight loss to Au(0) −60.91 %, found −59.95 %.

Dichlorido[*N*-dithiocarboxy-*kS*,$\kappa S'$-pyrrolidine]gold-(III) (Au^{III}Cl$_2$(PDT), 2) Yellow ochre powder (85.3 %): soluble in DMSO, acetone, and DMF, slightly soluble in CH$_3$CN and CH$_2$Cl$_2$, insoluble in H$_2$O, EtOH, MeOH, isopropanol, CCl$_4$, and diethyl ether; FT-IR (KBr): $\tilde{v}_{max} = 2980–2866$ (v, CH$_2$), 1586 (v, N–CSS), 1439 (v, CH$_2$), 942 cm^{-1} (v_a, S–C–S); FT-IR (Nujol): $\tilde{v}_{max} = 538$ (v_s, S–C–S), 413 (v_a, S–Au–S), 375 (v_s, S–Au–S), 362 (v_a, Cl–Au–Cl), 315 cm^{-1} (v_s, Cl–Au–Cl); ^{1}H NMR (300.13 MHz , [D$_6$]DMSO, 298 K): $\delta = 2.06$ (m, 4H, CH_2CH$_2$N), 3.82 ppm (m, 4H, CH$_2$N); ^{13}C NMR (75.48 MHz, [D$_6$]DMSO, 298 K): $\delta = 23.41$ (CH$_2$CH$_2$N), 51.10 (CH$_2$N), 188.58 ppm (CSS); Anal. calcd for C$_5$H$_8$AuCl$_2$NS$_2$ (MW = 412.13): C 14.50, H 1.95,

Cell viability assay

Cell viability was measured using the Resazurin-based In Vitro Toxicology Assay Kit (Sigma-Aldrich, St. Louis, USA). Cells (40,000/well) were plated into 96-well microplates the day before the experiment. After the 3 h treatments with compounds **1** or **2**, the Resazurin-based reagent was added. Then, cells were maintained at 37 °C for an additional 2 h, and the absorbance at 595 nm was detected using the iMark microplate reader (BioRad, Hercules, USA). All treatments were carried out in DMEM supplemented with L-Glutamine (Euroclone), penicillin (100 U mL^{-1}, Euroclone), and streptomycin (100 µg mL^{-1}, Euroclone) distributed into each well (200 µL) of a 96-well cell culture plate. Stock solutions of all complexes were made in DMSO and then diluted with complete medium in such a way that the final amount of solvent in each well did not exceed 0.4% (*v/v*). Cytotoxicity data were expressed as IC$_{50}$ values (Table 5), that is the concentration of the complex inducing a 50% decrease in cell number compared with control cultures.

ROS measurements

ROS measurements were performed using the probe 5-(and-6)-chloromethyl-2′,7′-dichlorodihydrofluorescein diacetate, acetyl ester (CM-H$_2$DCFDA, 1 µM, Molecular Probes, Carlsbad, USA). Cells (10,000/well) were plated the day before the experiment, and CM-H$_2$DCFDA was added with treatments in DMEM supplemented with 0.5% fetal bovine serum (FBS) without bicarbonate. Cells were maintained at 37 °C without CO$_2$ during the experiment, and the fluorescence ($\lambda_{ex} = 485$ nm, $\lambda_{em} = 538$ nm) was recorded using a Fluoroskan Ascent FL plate reader (Thermo Fisher Scientific, Waltham, USA) at different time points.

Measurement of mitochondrial Ca^{2+} retention capacity

The CRC assay was used to assess PTP opening by following trains of Ca^{2+} pulses which were measured fluorimetrically at 25 °C in the presence of the Ca^{2+} indicator Calcium Green-5N (1 µM, $\lambda_{ex} = 505$ nm, $\lambda_{em} = 535$ nm, Molecular Probes). We performed CRC experiments either on isolated mitochondria or on whole cells placed in an isotonic buffer (130 µM KCl, 1 µM Pi-Tris (Pi: inorganic phosphate), 10 mM Tris/3-(N-morpholino)propansulfonic acid (MOPS), 10 mM Tris/ethylene glycol tetraacetic acid (EGTA), 5 mM glutamate/2.5 mM malate, pH 7.4). Whole-cell CRC was carried out after 3 h treatment with compound **1**, followed by the plasma membrane permeabilization with the nonionic detergent digitonin, which is highly selective for cholesterol-enriched membranes and does not damage the mitochondrial membranes. Cells were washed with phosphate-buffered saline (PBS, pH 7.4) and then permeabilized with 150 µM digitonin (15 min, 4 °C) in a buffer composed of 130 µM KCl, 1 µM Pi-Tris, 10 mM Tris/MOPS, and 1 mM Tris/EGTA (pH 7.4). Digitonin was then washed away by spinning cells in the same buffer (15,000 rpm, 30 min) and changing the EGTA/Tris concentration to 0.1 mM, and the number of cells was carefully assessed before starting each experiment. Mitochondria (0.5 mg mL^{-1}) or permeabilized cells (7×10^6 cells per experiment) were then placed in the presence of the Ca^{2+} indicator Calcium-Green-5N, which does not permeate mitochondria, and were exposed to Ca^{2+} spikes (10 µM and 5 µM, respectively). Drops in fluo-rescence were used to assess mitochondrial Ca^{2+} uptake. PTP opening was detected as an increase in fluorescence. Pore inhibitors, such as cyclosporine A, are expected to enhance the threshold of Ca^{2+} concentration required to trigger the permeability transition, that is, the number of spikes before a sudden and marked fluorescence increase occurs.

[1] B. Rosenberg, L. Van Camp, T. Krigas, *Nature* **1965**, *205*, 698–699.
[2] K. D. Mjos, C. Orvig, *Chem. Rev.* **2014**, *114*, 4540–4563.
[3] B. Lippert, *Coord. Chem. Rev.* **1999**, *182*, 263–295.
[4] R. A. Alderden, M. D. Hall, T. W. Hambley, *J. Chem. Educ.* **2006**, *83*, 728–734.
[5] A. Casini, G. Kelter, C. Gabbiani, M. A. Cinellu, G. Minghetti, D. Fregona, H. H. Fiebig, L. Messori, *J. Biol. Inorg. Chem.* **2009**, *14*, 1139–1149.
[6] B. Biersack, A. Ahmad, F. H. Sarkar, R. Schobert, *Curr. Med. Chem.* **2012**, *19*, 3949–3956.
[7] G. Colotti, A. Ilari, A. Boffi, V. Morea, *Mini-Rev. Med. Chem.* **2013**, *13*, 211–221.
[8] U. Jungwirth, C. R. Kowol, B. K. Keppler, C. G. Hartinger, W. Berger, P. Heffeter, *Antioxid. Redox Signaling* **2011**, *15*, 1085–1127.
[9] A. Casini, L. Messori, *Curr. Top. Med. Chem.* **2011**, *11*, 2647–2660.
[10] N. P. E. Barry, P. J. Sadler, *Chem. Commun.* **2013**, *49*, 5106–5131.
[11] A. de Almeida, B. L. Oliveira, J. D. G. Correia, G. Soveral, A. Casini, *Coord. Chem. Rev.* **2013**, *257*, 2689–2704.
[12] E. Márta Nagy, L. Ronconi, C. Nardon, D. Fregona, *Mini-Rev. Med. Chem.* **2012**, *12*, 1216–1229.
[13] E. M. Nagy, A. Pettenuzzo, G. Boscutti, L. Marchiò, L. Dalla Via, D. Fregona, *Chem. Eur. J.* **2012**, *18*, 14464–14472.
[14] E. M. Nagy, C. Nardon, L. Giovagnini, L. Marchiò, A. Trevisan, D. Fregona, *Dalton Trans.* **2011**, *40*, 11885–11895.
[15] L. Kelland, *Nat. Rev. Cancer* **2007**, *7*, 573–584.
[16] B. Köberle, M. T. Tomicic, S. Usanova, B. Kaina, *Biochim. et Biophys. Acta - Rev. on Cancer* **2010**, *1806*, 172–182.
[17] J. Reedijk, *Plat. Met. Rev.* **2008**, *52*, 2–11.
[18] www.cancer.gov/cancertopics/druginfo/fda.
[19] L. Ronconi, D. Fregona, *Dalton Trans.* **2009**, 10670–10680.
[20] C. Nardon, G. Boscutti, D. Fregona, *Anticancer Res.* **2014**, *34*, 487–492.
[21] L. Ronconi, C. Nardon, G. Boscutti, D. Fregona in *Advances in Anti-Cancer Agents in Medicinal Chemistry, Vol. 2* (Ed.: M. Prudhomme), Bentham Science Publishers, Bussum, **2013**, chap. 3, pp. 130–172.
[22] C. Nardon, S. M. Schmitt, H. Yang, J. Zuo, D. Fregona, Q. P. Dou, *PLoS ONE* **2014**, *9*, e84248.
[23] V. Milacic, D. Chen, L. Ronconi, K. R. Landis-Piwowar, D. Fregona, Q. P. Dou, *Cancer Res.* **2006**, *66*, 10478–10486.

[24] M. Negom Kouodom, L. Ronconi, M. Celegato, C. Nardon, L. Marchiò, Q. P. Dou, D. Aldinucci, F. Formaggio, D. Fregona, *J. Med. Chem.* **2012**, *55*, 2212–2226.

[25] C. Marzano, L. Ronconi, F. Chiara, M. C. Giron, I. Faustinelli, P. Cristofori, A. Trevisan, D. Fregona, *Int. J. Cancer* **2011**, *129*, 487–496.

[26] L. Cattaruzza, D. Fregona, M. Mongiat, L. Ronconi, A. Fassina, A. Colombatti, D. Aldinucci, *Int. J. Cancer* **2011**, *128*, 206–215.

[27] L. Giovagnini, S. Sitran, M. Montopoli, L. Caparrotta, M. Corsini, C. Rosani, P. Zanello, Q. P. Dou, D. Fregona, *Inorg. Chem.* **2008**, *47*, 6336–6343.

[28] V. Milacic, D. Chen, L. Giovagnini, A. Diez, D. Fregona, Q. P. Dou, *Toxicol. Appl. Pharmacol.* **2008**, *231*, 24–33.

[29] J. J. Criado, J. A. Lopez-Arias, B. Macias, L. R. Fernandez-Lago, J. M. Salas, *Inorg. Chim. Acta* **1992**, *193*, 229–235.

[30] J. J. Criado, I. Fernandez, B. Macias, J. M. Salas, M. Medarde, *Inorg. Chim. Acta* **1990**, *174*, 67–75.

[31] J. J. Criado, A. Carrasco, B. Macias, J. M. Salas, M. Medarde, M. Castillo, *Inorg. Chim. Acta* **1989**, *160*, 37–42.

[32] B. Macías, J. J. Criado, M. V. Vaquero, M. V. Villa, *Thermochim. Acta* **1993**, *223*, 213–221.

[33] M. Castillo, J. J. Criado, B. Macias, M. V. Vaquero, *Inorg. Chim. Acta* **1986**, *124*, 127–132.

[34] D. A. Brown, W. K. Glass, M. A. Burke, *Spectrochim. Acta Part A* **1976**, *32*, 137.

[35] H. Ito, J. Fujita, K. Saito, *Bull. Chem. Soc. Jpn.* **1967**, *40*, 2584–2591.

[36] L. Gianelli, V. Amendola, L. Fabbrizzi, P. Pallavicini, G. G. Mellerio, *Rapid Commun. Mass Spectrom.* **2001**, *15*, 2347–2353.

[37] P. Bishop, P. Marsh, A. K. Brisdon, B. J. Brisdon, M. F. Mahon, *J. Chem. Soc. Dalton Trans.* **1998**, 675–682.

[38] F. Forghieri, C. Preti, L. Tassi, G. Tosi, *Polyhedron* **1988**, *7*, 1231–1237.

[39] U. Casellato, G. Fracasso, R. Graziani, L. Sindellari, A. S. González, M. Nicolini, *Inorg. Chim. Acta* **1990**, *167*, 21–24.

[40] D. J. Radanovic, Z. D. Matović, V. D. Miletić, L. P. Battaglia, S. Ianelli, I. A. Efimenko, G. Ponticelli, *Transition Met. Chem.* **1996**, *21*, 169–175.

[41] H. O. Desseyn, A. C. Fabretti, F. Forghieri, C. Preti, *Spectrochim. Acta Part A* **1985**, *41*, 1105–1108.

[42] L. Ronconi, L. Giovagnini, C. Marzano, F. Bettìo, R. Graziani, G. Pilloni, D. Fregona, *Inorg. Chem.* **2005**, *44*, 1867–1881.

[43] P. T. Beurskens, H. J. A. Blaauw, J. A. Cras, J. J. Steggerda, *Inorg. Chem.* **1968**, *7*, 805–810.

[44] G. E. Coates, C. Parkin, *J. Chem. Soc.* **1963**, 421–429.

[45] A. W. M. Lee, W. H. Chan, M. F. Ho, *Anal. Chim. Acta* **1991**, *246*, 443–445.

[46] G. C. Franchini, A. Giusti, C. Preti, L. Tassi, P. Zannini, *Polyhedron* **1985**, *4*, 1553–1558.

[47] C. C. Hadjikostas, G. A. Katsoulos, S. K. Shakhatreh, *Inorg. Chim. Acta* **1987**, *133*, 129–132.

[48] A. K. Gangopadhayay, A. Chakravorty, *J. Chem. Phys.* **1961**, *35*, 2206–2209.

[49] L. Ronconi, C. Marzano, P. Zanello, M. Corsini, G. Miolo, C. Maccà, A. Trevisan, D. Fregona, *J. Med. Chem.* **2006**, *49*, 1648–1657.

[50] L. Messori, F. Abbate, G. Marcon, P. Orioli, M. Fontani, E. Mini, T. Mazzei, S. Carotti, T. O'Connell, P. Zanello, *J. Med. Chem.* **2000**, *43*, 3541–3548.

[51] F. A. Cotton, G. Wilkinson, *Advanced Inorganic Chemistry, A Comprehensive Text, 3rd ed.*, Interscience, New York, **1972**, p. 1145.

[52] F. Chiara, A. Gambalunga, M. Sciacovelli, A. Nicolli, L. Ronconi, D. Fregona, P. Bernardi, A. Rasola, A. Trevisan, *Cell Death Dis.* **2012**, *3*, e444.

[53] A. Rasola, P. Bernardi, *Apoptosis* **2007**, *12*, 815–833.

[54] A. Rasola, P. Bernardi, *Cell Calcium* **2011**, *50*, 222–233.

[55] A. B. Trovó-Marqui, E. H. Tajara, *Clin. Genet.* **2006**, *70*, 1–13.

[56] S. Schubert, K. Shannon, G. Bollag, *Nat. Rev. Cancer* **2007**, *7*, 295–308.

[57] H. Brems, E. Beert, T. de Ravel, E. Legius, *Lancet Oncol.* **2009**, *10*, 508–515.

[58] F. Chiara, D. Castellaro, O. Marin, V. Petronilli, W. S. Brusilow, M. Juhaszova, S. J. Sollott, M. Forte, P. Bernardi, A. Rasola, *PLoS ONE* **2008**, *3*, e1852.

[59] D. Saggioro, M. P. Rigobello, L. Paloschi, A. Folda, S. A. Moggach, S. Parsons, L. Ronconi, D. Fregona, A. Bindoli, *Chem. Biol.* **2007**, *14*, 1128–1139.

[60] C. Frezza, E. Gottlieb, *Semin. Cancer Biol.* **2009**, *19*, 4–11.

[61] A. J. Levine, A. M. Puzio-Kuter, *Science* **2010**, *330*, 1340–1344.

[62] O. Warburg, *Science* **1956**, *123*, 309–314.

[63] M. P. Murphy, *Biochem. J.* **2009**, *417*, 1–13.

[64] R. A. Cairns, I. S. Harris, T. W. Mak, *Nat. Rev. Cancer* **2011**, *11*, 85–95.